2019 IEEE 58th Conference on Decision and Control (CDC)
Palais des Congrès et des Expositions Nice Acropolis
Nice, France, December 11-13, 2019

Lumped port–Hamiltonian burning plasma control model

Benjamin Vincent, Remy Nouailletas, Jean-François Artaud,
Nicolas Hudon, Laurent Lefèvre and Denis Dochain

Abstract— **In this contribution, we apply a spatial structure–preserving discretization scheme to a 1–D burning plasma model. The plasma dynamics are defined by a set of coupled conservation laws evolving in different physical domains, matching the port–Hamiltonian formalism in infinite dimension. This model describes the time evolution of magnetic, thermic, and material plasma profiles. A structure–preserving spectral collocation method is used to discretize the set of Partial Differential Equations (PDEs) into a finite–dimensional port–Hamiltonian system, a set of Ordinary Differential Equations (ODEs). The discretization scheme relies on the conservation of energy, based upon the transformation of Stokes–Dirac structures onto Dirac ones. Transport models and couplings are chosen to match with the experimental Tokamak ITER. Among the couplings, we include bootstrap and ohmic currents, ion–electron collision energy, radiation loses, and the fusion reaction. The obtained control model is compared with two steady–state operation points obtained from a physics–oriented plasma simulator.**

I. Introduction

In this paper, we are interested in the derivation of a finite–dimensional (lumped) structured port–Hamiltonian control burning plasma model. A special attention is given to the considered geometric preserving spatial discretization scheme. This contribution follows the modelling stage of control structured burning plasma port–Hamiltonian models initiated in [11] and [12], where a 3–D port–Hamiltonian model was geometrically reduced into a 1–D one. The spatial reduction relied on the quasi–static plasma equilibrium of the momentum balance equation and the assumption of axial symmetry of the plasma [1]. The structure–preserving method provides us a 1–D burning plasma control model. Lumped models enable us to validate control models, to develop, and, to implement control laws [15].

Tokamaks are experimental toroidal shaped devices in which the fuel reaches high energy levels and takes the form a plasma [16]. Plasma profile control remains a key step toward the operation of a future carbon free energy production device without nuclear waste. Tokamak plasmas are modelled by a set of balance equations governing the electromagnetic and kinetic physical domains. Indeed, in the proposed model, Maxwell's laws are describing the electric and magnetic fields while mass, momentum, and energy balance equations are governing the particle density and temperature profiles. Infinite–dimensional systems described by balance equations can be represented within the port–Hamiltonian framework [9]. A proof of concept for magnetic plasma profile control within the port–Hamiltonian framework was proposed in [15]. We are now extending the plasma model to burning plasmas by including the fusion reaction and the species balance equations. The cornerstone of plasma model resides in the selected closure equations and couplings equations from which nonlinearities arise. Transport coefficients depend on the state variables and the plasma geometry [1]. Distributed sources/sink terms in the balance equations are modelled by nonlinear relations expressed mostly by scaling laws. Among the couplings, we considered bootstrap and ohmic currents, ion–electron collision energy, radiation losses and the fusion reaction. With this model, we can address control issues for full power steady–state operation of the future experimental Tokamak ITER [4].

The discretization method applied here preserves the spectrum properties [14]. The discretization technique is based on the approximation of effort and flow variables in appropriate spaces such that the exact derivation is known, and the product of effort and flow variables (the power) is exactly computed [6]. The discretization method is applied to all balance equations defining the plasma dynamics. Numerical results obtained from the proposed model are compared with METIS simulation data [5]. The control model is compared with two ITER steady–state operation points, defined by a total plasma current of 9 and 15 mega–amperes.

The paper is structured as follows. In section II, the 1–D burning plasma model is recall. Section III is dedicated to the presentation of the spatial discretization scheme. In section IV the lumped burning plasma control model is derived and compared with two experimental steady–state operation scenarios.

II. 1–D structured burning plasma model

Under the quasi–static equilibrium and axial symmetry assumptions, the plasma is structured as nested magnetic surfaces [1]. Each surface are indexed by a radial toroidal flux coordinate $\rho = \sqrt{\Phi/(\pi B_0)}$, where Φ is the toroidal magnetic flux, B_0 the vacuum magnetic field at the major radius R_0. We assume in the following that Φ is given. A normalized coordinate system $z \in \Pi = [0,\ 1]$ is adopted

B. Vincent and D. Dochain are with ICTEAM, Université Catholique de Louvain, Bâtiment Euler, av. Lemaître 4-6, B-1348 Louvain-La-Neuve, Belgium. e-mail:{benjamin.vincent, denis.dochain}@uclouvain.be

B. V. and L. L. are with Université Grenoble Alpes, LCIS, F-26902, France. e-mail:laurent.lefevre@lcis.grenoble-inp.fr

N. Hudon is with Department of Chemical Engineering, Queen's University, Kingston, ON, K7L 3N6 Canada. e-mail: nicolas.hudon@queensu.ca

R. Nouailletas and J.-F. Artaud are with CEA, IRFM, F-13108 Saint-Paul-Lez-Durance, France. (e-mail:{remy.nouailletas, Jean-Francois.artaud}@cea.fr)

and plasma dynamics are defined by 1–D partial differential equations for the electro–magnetic, heat, and particle transport equations. A linear Stokes–Dirac structures can be identified in these balance equations. We recall here the model proposed in [12]. The system is composed of five balances equations: one for the magnetic field, two for the internal energy (electron and ion temperature profiles are different), and two for the particles (one for the electrons and one for the helium, the product of the fusion reaction).

A. Electro–magnetic part

The 1–D reduced Maxwell's equations govern the electro–magnetic part of the plasma dynamics and take the following form:

$$\begin{pmatrix} f_1 \\ f_2 \end{pmatrix} = \begin{pmatrix} 0 & -\frac{\partial}{\partial z} \\ -\frac{\partial}{\partial z} & 0 \end{pmatrix} \begin{pmatrix} e_1 \\ e_2 \end{pmatrix} - \begin{pmatrix} 1 \\ 0 \end{pmatrix} f_d, \qquad (1)$$

where $f_1 = -\partial_t \overline{D}_\phi$, $f_2 = -\partial_t \overline{B}_\theta$, $e_1 = \overline{E}_\phi$, $e_2 = \overline{H}_\theta$, and $f_d = \overline{J}_\phi$. $\overline{B}$, $\overline{D}$, $\overline{E}$, $\overline{H}$, and $\overline{J}$ denote the magnetic flux, the electric flux, the electric field and the magnetic fields, and the current density, respectively. Subscripts ϕ and θ denote the poloidal and toroidal components of a variable. The balance equation is closed with the Ampere's law:

$$e_2 = \frac{C_2(t,z)}{\mu_0} \overline{B}_\theta, \qquad (2)$$

where μ_0 is the vacuum permeability, and the Ohm's law:

$$e_1 = \eta(t,z) C_3(t,z) \overline{J}_{\text{ohm}}, \qquad (3)$$

where $\eta(t,z)$ represents the plasma resistivity. The ohmic current $\overline{J}_{\text{ohm}}$ is the difference between the current $\overline{J}_\phi$ and the non–inductive one $\overline{J}_{\text{ni}}$. The current $\overline{J}_\phi$ is the reduced 1–D non–inductive plasma current. The non–inductive current is the sum of all external currents $\overline{J}_{\text{ext}}$ and the bootstrap current is denoted $\overline{J}_{\text{bt}}$ (see section IV-D, or [16]). The total plasma current $\overline{J}_{\text{tot}}$ is the sum of the ohmic current $\overline{J}_{\text{ohm}}$ and the non–inductive one $\overline{J}_\phi$, that includes couplings and input source terms. Boundary conditions are as follows:

$$f_2 = z|_{z=0} = 0, \qquad e_1|_{z=1} = V_{\text{loop}}(t) \in \mathbb{R}. \qquad (4)$$

The first condition expresses the symmetry at the plasma center and the second is the plasma loop voltage, a control input. Geometric coefficients C_2 and C_3 are known and defined in [1].

Remark 1: Under the assumption that $\overline{D}_\phi$ is at steady–state (the displacement current is small compared to the inductive current), model (1) is equivalent to the resistive diffusion equation [17]:

$$\frac{\partial \psi}{\partial t} = \eta(t,z) \frac{1}{C_3} \frac{\partial}{\partial z} \left(\frac{1}{\mu_0} C_2 \frac{\partial \psi}{\partial z} \right) + \frac{1}{C_3} \left(\eta(t,z) \overline{J}_{\text{ni}} \right), \quad (5)$$

with $\psi(t,z)$ the poloidal magnetic flux defined such that $\overline{B}_\theta = -\frac{\partial \psi}{\partial z}$ and $\frac{\partial \psi}{\partial t} = \overline{E}_\phi$. Boundary conditions (4) are retrieved:

$$\left. \frac{\partial \psi}{\partial z} \right|_{z=0} = 0, \qquad \text{and,} \qquad \left. \frac{\partial \psi}{\partial t} \right|_{z=1} = V_{\text{loop}}(t). \qquad (6)$$

B. Kinetic part

The plasma kinetic part is described by mass and internal energy balance equations. The following particles are present: electrons, deuterium, tritium, helium, impurities (required for realistic radiation losses). Under the plasma quasi–neutrality assumption, particle densities are subject to the following constraints $n_e(t,z) Z_{\text{eff}}(t,z) = \sum_k Z_k^2 n_k(t,z)$ and $n_e(t,z) = \sum_k Z_k n_k(t,z)$, where sums are carried over all ion species, and, $Z_{\text{eff}}(t,z)$ denotes the plasma effective charge. Furthermore, we assume equipartition of deuterium and tritium within the plasma. We thus consider two particle balance equations, one for the electron and one for the helium.

1) Heat transport equation for electrons and ions: The internal energy balance equation of a particle a (electron or ion) is given as an implicit Stokes–Dirac structure of the form

$$\begin{pmatrix} f_1 \\ e_2 \end{pmatrix} = \begin{pmatrix} 0 & -\frac{\partial}{\partial z} \\ -\frac{\partial}{\partial z} & 0 \end{pmatrix} \begin{pmatrix} e_1 \\ f_2 \end{pmatrix} + \begin{pmatrix} 1 \\ 0 \end{pmatrix} f_d \qquad (7)$$

where $f_1 = \partial e_a / \partial t$, $f_2 = q_a$, $e_1 = T_a$, $e_2 = -\partial T_a / \partial z$, and $f_d = V' \overline{Q}_a$ denote the time derivative of the internal energy, the heat flux, the temperature profile, the temperature gradient, and the distributed internal energy source/sink term, respectively. By definition, the internal energy is $e_a V' \frac{3}{2} n_a T_a$. The geometric coefficient $V'(t,z)$ denotes the spatial derivative with respect to the spatial coordinate of the plasma volume $V(t,z)$. The heat flux $q_a(t,z)$ is assumed to be driven by the temperature gradient such that

$$q_a(t,z) = G_1 n_a \chi_a \frac{\partial T_a}{\partial z}, \qquad (8)$$

where $G_1(t,z)$ is a known geometric coefficient, and $\chi_a(t,z)$ represents the heat diffusion flux transport coefficient. The heat transport equation is subject to the following boundary conditions

$$\left. \frac{\partial T_a}{\partial z} \right|_{z=0} = 0, \qquad \text{and} \qquad T_a(t,1) = T_{a1} \in \mathbb{R}, \qquad (9)$$

where the first condition expresses the plasma symmetry and the second is the plasma edge temperature. The conservation law associated to (7) is

$$\frac{\partial e_a}{\partial t} = \frac{\partial}{\partial z} \left(V' q_a \right) + V' \overline{Q}_a. \qquad (10)$$

Remark 2: Two temperature profiles are considered, one for ions and one for electrons. An alternative approach would be to introduce an average temperature as in [17] and [13]. Since both temperature dynamics are governed by conservation laws, the methodology remains the same for both equations. The ion temperature is the average temperature of all ions (helium, deuterium and tritium).
The source terms vary with the species a: for ions $\overline{Q}_i = \overline{Q}_{e,i} + \overline{Q}_{\text{fus},i} + \overline{Q}_{\text{ext},i}$, respectively, the ion electron collisional energy transfer, fusion, and, external sources; for electrons $\overline{Q}_e = -\overline{Q}_{e,i} + \overline{Q}_{\text{ohm}} - \overline{Q}_{rad} + \overline{Q}_{\text{fus},e} + \overline{Q}_{\text{ext},e}$, where contributions results from ion–electron energy transfer, ohmic source, radiation losses, fusion reaction and external sources, respectively. More details are provided in [5].

2) Particle conservation laws: Reduced 1–D particle balance equations take the form of parabolic equations:

$$V' \frac{\partial n_a}{\partial t} = \frac{\partial}{\partial z}\left(V' \Gamma_a \right) + V' \overline{P}_a, \tag{11}$$

where $n_a(t,z)$ and $\overline{P}_a$ denote the particle density profile, and the density distributed source term, respectively, and gather all external sources of particles. The particle flux is modelled as a diffusion process:

$$\Gamma_a(t,z) = G_1 D_a \frac{\partial n_a}{\partial z}, \tag{12}$$

where D_a denotes the particle diffusion transport coefficient. Equation (11) is subject to the following boundary conditions

$$\left.\frac{\partial n_a}{\partial z}\right|_{z=0} = 0, \qquad \text{and} \qquad n_a(t,1) = n_{a1} \in \mathbb{R}, \tag{13}$$

where n_{a1} is the particle density at the plasma edge. Particle diffusion equations (11) are defined by the same implicit Stokes–Dirac structure as the heat transport equation (7), where coefficients are: $f_1 = \partial(V' n_a)/\partial t$, $f_2 = \Gamma_a$, $e_1 = n_a$, $e_2 = -\partial n_a/\partial z$, and $f_d = V' \overline{P}_a$. Particle source terms result from the contribution of the fusion reaction, and the external inputs terms: pellet injections or gas puffing [5].

C. Transport and couplings

Subsystems are coupled through nonlinear distributed transport coefficients and source terms. A diagonal transport model is privileged [10], and transport coefficients are defined as follows.

- The plasma resistivity $\eta(t,z)$ is modelled according to neoclassical theory [8]. This parameter is a function of the plasma toroidal magnetic profile and of the electron temperature.
- The plasma ion thermal diffusion coefficient is defined according to the Chang–Hinton formula [16]. This model is valid for different transport regimes and take into account impurities. This transport coefficient is a function of the toroidal magnetic profile and temperature profiles. The electron thermal diffusivity coefficient is proportional to the ion one.

Nonlinear sinks/sources coupling terms include the followings phenomena.

- The bootstrap current density $\overline{J}_{\text{bt}}$ results from neoclassical transport of trapped particles and is a non–inductive current source [8]. This current is nonlinear, driven by temperature and density gradient profiles, and is inversely proportional to the poloidal magnetic flux.
- The ohmic heating results from the plasma resistivity (Joule effect) and is defined as $\overline{Q}_{\text{ohm}}(t,z) = \eta \overline{J}_{\text{tot}}(\overline{J}_{\text{tot}} - \overline{J}_{\text{ni}})$ where $\overline{J}_{\text{tot}}$ is the total plasma current density.
- The deuterium/tritium fusion reactivity, $\langle \sigma v \rangle_{DT}$, is modelled with a scaling law [2]. Particle fusion density and heat transport fusion source terms are defined as $\overline{P}_{\text{fus}}(t,z) = n_D(t,z) n_T(t,z) \langle \sigma v \rangle_{DT}$, and $\overline{Q}_{\text{fus}}(t,z) = e^- E_\alpha P_{\text{fus}}(t,z)$, respectively. The electron charge and the fusion energy associated to the Helium are denoted e^- and E_α, respectively.
- The Neutral Beam Injection (NBI) is a distributed actuator source of current density, heat and momentum. Here, we consider it to be a source of heat and current approximated by a Gaussian shape deposition profile [5]. Heat deposition is distributed to ions and electrons [16, equation 5.4.12].
- The Electron Cyclotron Current Drive and Radio-frequency Heating (ECCD/ECRH) and Ion Cyclotron Current Drive and Radio-frequency Heating (ICCD/ICRH) provide external source of current and heating for electrons and ions, respectively. In both cases, the actuator deposition shape are approximated by Gaussian curves [5].
- The radiation heating sink terms combine Line and Bremsstrahlung losses. The model is similar to the one used in [5].
- The pellet injection is assumed to be defined by a Gaussian deposition shape profile.

A complete review of current, heating and particle actuators can be found in the monograph [16].

III. Structure preserving discretization

The spatial discretization procedure allows to express the infinite–dimensional system into a finite–dimensional one [6]. This discretization conserves the model structure. The idea is to project the effort and flow variables in two different approximation spaces:

$$\begin{aligned} f(t,z) &= \sum_{k=1}^{N-1} (\mathbf{f}(t))_k w_k^f(z), \\ e(t,z) &= \sum_{i=1}^{N} (\mathbf{e}(t))_i w_k^e(z), \end{aligned} \tag{14}$$

where $\mathbf{f}(t) \in \mathbb{R}^{N-1}$ and $\mathbf{e}(t) \in \mathbb{R}^N$ are time–dependent coefficients. $w^f(z)$ and $w^e(z)$ are base functions defined in spaces $\overline{\mathcal{E}} = \text{span}(w_i^e(z))$ and $\overline{\mathcal{F}} = \text{span}(w_i^f(z))$, respectively, such that $d(\overline{\mathcal{E}}) = \overline{\mathcal{F}}$. After the reduction, the original Stokes–Dirac structure becomes a Dirac structure [6]. The exact differentiation implies the following condition on the effort and flow vector time variables $\mathbf{f}(t)$ and $\mathbf{e}(t)$:

$$\mathbf{f}(t) = D\mathbf{e}(t), \tag{15}$$

where $D \in \mathbb{R}^{(N-1)\times N}$ denotes the differentiation matrix. Efforts and flows are not of the same dimension (N and $N-1$), therefore we introduce a projected effort $\tilde{\mathbf{e}}$

$$\tilde{\mathbf{e}} = M^\top \mathbf{e} \tag{16}$$

such that the power balance is non–degenerate:

$$\frac{\partial \mathbb{H}}{\partial t} = \int_\Pi e(t) \cdot f(t) = \mathbf{e}(t)^\top M \mathbf{f}(t) = \tilde{\mathbf{e}}(t)^\top \mathbf{f}(t). \tag{17}$$

Replacing all projected efforts and flows in the 1–D Stokes–Dirac structure, one gets:

$$\begin{pmatrix} f_p \\ f_q \end{pmatrix} = \begin{pmatrix} 0 & -D \\ -D & 0 \end{pmatrix} \begin{pmatrix} e_p \\ e_q \end{pmatrix}, \quad \begin{pmatrix} f_{1p} \\ f_{0q} \\ e_{1p} \\ e_{0q} \end{pmatrix} = \begin{pmatrix} w^e(1) & 0 \\ w^e(0) & 0 \\ 0 & w^e(1) \\ 0 & w^e(0) \end{pmatrix} \begin{pmatrix} e_p \\ e_q \end{pmatrix}. \tag{18}$$

Injecting the projected efforts (16) in the structure, the following Dirac structure is identified:

$$\begin{bmatrix} \begin{pmatrix} f_p \\ e_{1q} \end{pmatrix} \\ \begin{pmatrix} f_q \\ -e_{0p} \end{pmatrix} \end{bmatrix} = \mathcal{J} \begin{bmatrix} \begin{pmatrix} \tilde{e}_p \\ f_{1p} \end{pmatrix} \\ \begin{pmatrix} \tilde{e}_q \\ e_{0q} \end{pmatrix} \end{bmatrix}, \tag{19}$$

where the interconnection matrix is defined by

$$\mathcal{J} = \begin{bmatrix} 0_{N\times N} & \begin{pmatrix} -D \\ w^e(1) \end{pmatrix} \begin{pmatrix} M^\top \\ w^e(0) \end{pmatrix}^{-1} \\ \begin{pmatrix} -D \\ -w^e(0) \end{pmatrix} \begin{pmatrix} M^\top \\ w^e(1) \end{pmatrix}^{-1} & 0_{N\times N} \end{bmatrix},$$

and satisfies $\mathcal{J} = -\mathcal{J}^\top$. The reduced finite–dimensional version of Stokes–Dirac theorem in the conjugated approximation spaces for the reduced effort and flow variables is given by:

$$MD + D^\top M^\top - T_1 + T_0 = 0, \tag{20}$$

where trace matrices $T_l \in \mathbb{R}^{N\times N}$, $l = \{0, 1\}$, are

$$(T_l)_{ik} = w_i^e(z = k) w_k^e(z = k). \tag{21}$$

In the case of homogeneous boundary conditions, efforts at the boundary and, by extension, the trace matrices, are given by $T_1 = T_0 = 0$. Homogeneous boundary conditions are integrated within the discretization scheme. Indeed, an appropriate choice of approximation basis function enables us to only consider functions satisfying the boundary conditions. For time–varying boundary conditions, they are directly interconnected to the effort and flow variables in the approximation bases in the finite–dimensional state–space model. Spatial distributed source terms and closure relations are expressed in the same approximation bases.

IV. Lumped control model

The previously presented discretization method is applied to the 1–D burning plasma model introduced in section II. Constitutive relations are reduced by projection of efforts and flows in the approximation basis and integrated over the spatial domain $\Pi = [0, 1]$.

A. Resistive diffusion equation

Magnetic and electric fields are projected such that

$$\overline{B}_\theta = \sum_{k=1}^{N-1} (\mathbf{b}(t))_k \omega_k^f(z), \tag{22}$$

and

$$\overline{D}_\phi = \sum_{k=1}^{N-1} (\mathbf{d}(t))_k \omega_k^f(z). \tag{23}$$

Bold variables $\mathbf{b}$, $\mathbf{d}$, and $\mathbf{j} \in \mathbb{R}^{N-1}$ denote time–varying coefficients for the electric, magnetic and current variables, respectively. The reduced port–Hamiltonian formulation of equation (1) is given as

$$\begin{pmatrix} \dot{\mathbf{d}} \\ \dot{\mathbf{b}} \end{pmatrix} = \left[\begin{pmatrix} 0 & \mathbf{J}_{\text{em}} \\ -\mathbf{J}_{\text{em}}^\top & 0 \end{pmatrix} - \begin{pmatrix} \mathbf{R}_{\text{em}}^{-1} & 0 \\ 0 & 0 \end{pmatrix} \right] \begin{pmatrix} \mathbf{G}_{\text{el}} \mathbf{d} \\ \mathbf{G}_{\text{mg}} \mathbf{b} \end{pmatrix} + \begin{pmatrix} -\mathbf{j}_{\text{ni}} \\ \mathbf{J}_{\text{b}} V_{\text{loop}} \end{pmatrix}, \tag{24}$$

where $\mathbf{J}_{\text{em}} = -\mathbf{J}_{\text{em}}^\top \in \mathbb{R}^{N-1} \times \mathbb{R}^{N-1}$ denotes the interconnection matrix, $\mathbf{R}_{\text{em}} \geq 0$ is the dissipative matrix which is function of the plasma resistivity $\eta(t, z)$, $\mathbf{G}_{\text{el}} = \mathbf{G}_{\text{el}}^\top \geq 0$ and $\mathbf{G}_{\text{mg}} = \mathbf{G}_{\text{mg}}^\top \geq 0$ are the energy storage matrices. Boundary control variable $V_{\text{loop}}(t)$ is mapped through the boundary input vector $\mathbf{J}_{\text{b}} \in \mathbb{R}^{N-1}$, while $\mathbf{j}_{\text{ni}}$ represents the distributed non–inductive current source term. The approximate electromagnetic energy is given by the quadratic function

$$\mathbb{H}(\mathbf{b}(t), \mathbf{d}(t)) = \frac{1}{2} \left(\mathbf{d}^\top(t) \mathbf{G}_{\text{el}} \mathbf{d}(t) + \mathbf{b}^\top(t) \mathbf{G}_{\text{mg}} \mathbf{b}(t) \right), \tag{25}$$

where the electric storage matrix $\mathbf{G}_{\text{el}} = \mathbf{G}_{\text{el}}^\top \geq 0$ is defined as

$$\mathbf{G}_{\text{el}_{ij}} = \int_\Pi \frac{1}{\varepsilon C_3} \omega_i^f(z) \omega_j^f(z) dz, \tag{26}$$

and $\mathbf{G}_{\text{mg}} = \mathbf{G}_{\text{mg}}^\top \geq 0$, the magnetic storage matrix, is derived from the Ampere's law (2) such that:

$$\mathbf{G}_{\text{mg}_{ij}} = \int_\Pi \frac{C_2}{\mu_0} \omega_i^f(z) \omega_j^f(z) dz. \tag{27}$$

The resistive element $\mathbf{R}_{\text{em}} = \mathbf{R}_{\text{em}}^\top \geq 0$ is derived from the Ohm's law (3) such that:

$$\mathbf{R}_{\text{em}_{ij}} = \int_\Pi \frac{\eta}{C_3} w_i^f(z) w_j^f(z) dz. \tag{28}$$

B. Heat diffusion equation

The discretized resistive heat diffusion equation is given by

$$\begin{pmatrix} \dot{\mathbf{e}}_a \\ 0 \end{pmatrix} = \left[\begin{pmatrix} 0 & \mathbf{J}_{e_a} \\ -\mathbf{J}_{e_a}^\top & 0 \end{pmatrix} - \begin{pmatrix} 0 & 0 \\ 0 & \mathbf{R}_{T_a}^{-1} \end{pmatrix} \right] \begin{pmatrix} \mathbf{G}_{T_a} \mathbf{e}_a \\ \mathbf{J}_{a,q} \end{pmatrix} + \begin{pmatrix} \overline{\mathbf{Q}}_a \\ \mathbf{J}_{a4} T_{a1} \end{pmatrix}, \tag{29}$$

where $\mathbf{e}_a(t) = V' \frac{3}{2} n_a T_a$, $\mathbf{J}_{\text{em}} = -\mathbf{J}_{\text{em}}^\top \in \mathbb{R}^{N-1} \times \mathbb{R}^{N-1}$ denotes the interconnection matrix, $\mathbf{R}_T = \mathbf{R}_T^\top \geq 0$ is the thermal dissipative matrix, and $\mathbf{G}_T = \mathbf{G}_T^\top \geq 0$ is the stored energy matrix. Note that the plasma boundary temperature T_{a1} is now included in the state equation (29) through the vector $\mathbf{J}_{a4} \in \mathbb{R}^{N-1}$. Internal energy source/sink terms are projected in the approximation basis and are gathered in the term $\overline{\mathbf{Q}}_a$. The internal energy for a species a is projected such that

$$e_a = \sum_{k=1}^{N-1} (\mathbf{e}_a(t))_k \, \omega_k^f(z). \tag{30}$$

Therefore the Hamiltonian function is defined by

$$\mathbb{H}_T(\mathbf{e}_a(t)) = \frac{1}{2} \mathbf{e}_a(t)^\top \mathbf{G}_{T_a} \mathbf{e}_a(t), \tag{31}$$

where the storage matrix $\mathbf{G}_{T_a} = \mathbf{G}_{T_a}^\top > 0$ is given by:

$$\mathbf{G}_{T_{a,ij}} = \int_\Pi \left(\frac{3}{2} n_a V'\right)^{-1} w_i^f(z) w_j^f(z) dz. \quad (32)$$

The resistivity matrix $\mathbf{R}_{T_a} = \mathbf{R}_{T_a}^\top > 0$ is defined by

$$\mathbf{R}_{T_{a,ij}} = \int_\Pi \chi_a n_a V' G_1 \omega_i^f(z) \omega_j^f(z) dz, \quad (33)$$

and is derived from the projection of Fourier's law (8) in the approximation basis.

C. Particle diffusion equation

The lumped formulation of the particle diffusion balance equation takes the following form:

$$V'\begin{pmatrix}\dot{\mathbf{n}}_a \\ 0\end{pmatrix} = \left[\begin{pmatrix}0 & \mathbf{J}_{n_a} \\ -\mathbf{J}_{n_a}^\top & 0\end{pmatrix} - \begin{pmatrix}0 & 0 \\ 0 & \mathbf{R}_{n_a}^{-1}\end{pmatrix}\right]\begin{pmatrix}\mathbf{G}_{n_a}\mathbf{n_a} \\ \mathbf{J}_{n_a}\end{pmatrix} + \begin{pmatrix}V'\overline{P}_a \\ \mathbf{J}_{4a} n_{a1}\end{pmatrix}, \quad (34)$$

where $\mathbf{n}_a(t)$ is the particle density time–varying coefficient associated to the chosen approximation basis, the plasma edge density is fixed by variable $n_{a1} = 0$. The electron density profile is projected as follows:

$$n_a = \sum_{k=1}^{N-1} (\mathbf{n}_a(t))_k \omega_k^f(z). \quad (35)$$

The Hamiltonian function associated to this sub–model takes the quadratic form

$$\mathbb{H}_{\mathbf{n}_a} = \frac{1}{2} \mathbf{n}_a(t)^\top \mathbf{G}_{n_a} \mathbf{n}_a(t), \quad (36)$$

where

$$\mathbf{G}_{n_{a,ij}} = \int_\Pi V' G_1 \omega_i^f(z) \omega_j^f(z) dz. \quad (37)$$

The dissipative element $\mathbf{R}_{n_a} = \mathbf{R}_{n_a}^\top > 0$ is defined by the following integral

$$\mathbf{R}_{n_{a,ij}} = \int_\Pi D_e G_1 \omega_i^f(z) \omega_j^f(z) dz, \quad (38)$$

where we retrieve the particle diffusion flux equation (12).

D. Coupled control model

The complete model is composed by the electro–magnetic component (24), the heat diffusion (29), and the particle diffusion equations (34). It generates a finite–dimensional port–control Hamiltonian system of the form

$$\dot{x} = [J - R] \frac{\partial H}{\partial x}(x) + g u, \quad (39)$$

with $J = -J^\top$ and $R = R^\top \geq 0$. The total Hamiltonian function being the sum of all Hamiltonians (25), (31) and (36). Boundary and distributed inputs are gathered in the last term in the right hand side of the state equation (39).

E. Sources and geometry

The discretized model include boundary coefficients with the loop voltage, V_{loop}, the plasma boundary temperature T_{a1}, and particle density n_{a1}. Reduced distributed source/sink terms $\mathbf{j}_{\text{ni}}$, $\mathbf{Q}_a$, and $\mathbf{P}_a$ are the projection of the reduced 1–D non–inductive current $\overline{J}_\phi$, distributed heat $V'\overline{\mathcal{Q}}_a$, and particle sources in the approximation basis $V'\overline{\mathcal{P}}_a$, respectively. The discretization scheme assumes the geometric coefficients C_2, C_3, G_1, and V' to be known.

F. Numerical results

A unique set of approximation functions is used for all state equations. First–order Bessel functions are defined as flow approximation bases, as they are eigenfunctions of the linear and homogeneous resistive diffusion equations (5), (10), and (11). This provide good eigenvalues approximation, with a low number of functions [14]. Resistive and conservative matrices derived in the reduced model are dependent on the appropriate transport coefficients η, χ and geometric coefficients C_2, C_3, G_1 and V'. With non–homogeneous distributed parameters, Bessel eigenfunctions are no longer solution of the resistive diffusion equations. Integral are computed with the Gauss quadrature formula at Chebyshev discretization points such that for a given function $f(x)$, one gets

$$\int_0^1 f(x) dx = \sum_{k=1}^m \omega_g(x_k) f(x_k), \quad (40)$$

where Chebyshev points are $x_k = \frac{1}{2}\left(1 - \cos\left(\frac{2k-1}{2(m-1)}\pi\right)\right)$ and the Gauss quadrature weights are given by

$$\omega_g(x_k) = \frac{\pi}{2m}\sqrt{1 - (1 - 2x_k)^2}. \quad (41)$$

The discretized model is evaluated for two ITER scenario at different plasma currents, $I_p = 9\ MA$, and $15\ MA$. By definition, the plasma current is proportional to the plasma current evaluated at its boundary [16]. Equilibria of the discretized model are compared with METIS simulation data. METIS is a physics–based oriented Tokamak plasma code [5]. Geometric coefficients are those provided and supposed to be constant with respect to time. Distributed sources, including heat deposition and current density profile, are provided by METIS. The loop voltage V_{loop} is controlled through a PI controller to fit the total plasma current $I_p(t)$. The number of approximation basis is set to $N = 6$, and Gauss–Chebyshev discretization points to $m = 200$. Figures 1 and 2 present the steady–state equilibrium profiles for $I_p = 9\ MA$, and $15\ MA$. The left side of each figure represents the magnetic profile B_θ and the safety factor profile q, and the equilibrium obtained by METIS. The safety factor profile is defined as $q = -1/(2\pi)\frac{\partial \Phi}{\partial \psi}$, and is an important quantity for advanced control problems [15].
The right sides of Figures 1 and 2 show the kinetic equilibrium profiles compared to the ones obtained in METIS. Plain and dotted lines represent our discretized model and METIS data, respectively. The reduced burning plasma model has different steady–state profiles even if their shape remains

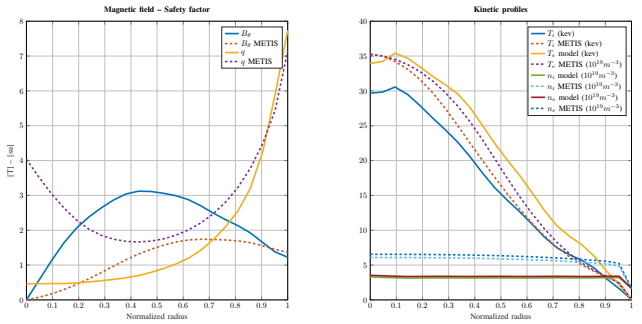

Fig. 1. Magnetic and safety factor profiles (left), and kinetic profiles (right) at steady–state for ITER scenario, $9MA$ of total plasma current, and average density $\overline{n} = 6,1e^{19}m^{-3}$

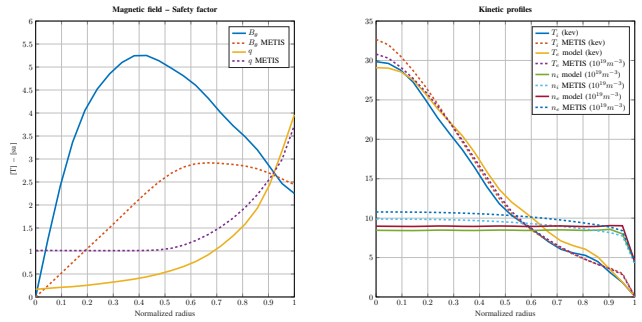

Fig. 2. Magnetic and safety factor profiles (left), and kinetic profiles (right) at steady–state for ITER scenario, $15\ MA$ of total plasma current, and average density $\overline{n} = 10e^{19}m^{-3}$

of the same order of magnitude. An approximated shape for the solution is enough as we are developing a control model. Non–included phenomena in the developed model justify the errors in the plasma profile equilibrium states. For example, sawtooth effects that tend to stabilize the plasma when a critical magnetic shear for $q = 1$ is achieved. The two equilibrium points of the discretized model are close enough to the plasma behaviour to consider as a next step the control of the total plasma fusion reaction [3].

V. Conclusion

In this contribution, we have presented and applied a structure–preserving discretization method for a burning plasma model. This model is described by a set of balance equations, formulated with Stokes–Dirac interconnection structure. The discretization scheme relies on the preservation of one invariant, the Hamiltonian function. The discretized model is compared with data–sets generated by METIS (a physics–oriented Tokamak plasma model) of two steady–state operational points of ITER plasma. Key design choice of the discretization method resides on the choice of basis functions. Here, we have set the effort functions as the eigenfunctions of the homogeneous resistive diffusion equation ruling the plasma model. The discretization scheme is independent of the choice of transport model, as long as the balance equations structure remains unchanged. The reduced structured burning plasma model provides good results at steady–state. The model validity resides in the choice of appropriate transport coefficients and couplings terms. We have used here state of the art transport models [5].

Ongoing work concerns the model dynamical validation around the equilibrium points, the inclusion of kinetic transport coefficients on the material balances equations, and the control of total fusion power of a burning plasma. Indeed, the derived model in the present contribution is a strong basis for future model based control, like IDA–PBC [7].

References

[1] J. Blum. *Numerical Simulation and Optimal Control in Plasma Physics: With Applications to Tokamaks*. Gauthier–Villars, New York, 1989.

[2] H. S. Bosch and G. M. Hale. Improved formulas for fusion cross–sections and thermal reactivities. *Nuclear fusion*, 32(4):611–631, 1992.

[3] M. D. Boyer and E. Schuster. Nonlinear burn condition control in tokamaks using isotopic fuel tailoring. *Nuclear Fusion*, 55(8):083021, 2015.

[4] D. Humphreys et al. Novel aspects of plasma control in ITER. *Physics of Plasmas*, 22(2):021806, 2015.

[5] J.F. Artaud et al. METIS: A fast integrated tokamak modelling tool for scenario design. *Nuclear Fusion*, 58(10):105001, 2018.

[6] R. Moulla, L. Lefèvre, and B. Maschke. Geometric pseudospectral method for spatial integration of dynamical systems. *Mathematical and Computer Modelling of Dynamical Systems*, 17(1):85–104, 2011.

[7] R. Ortega, A. van der Schaft, B. Maschke, and G. Escobar. Interconnection and damping assignment passivity–based control of port–controlled Hamiltonian systems. *Automatica*, 38(4):585 – 596, 2002.

[8] O. Sauter, C. Angioni, and Y. R. Lin-Liu. Erratum: "Neoclassical conductivity and bootstrap current formulas for general axisymmetric equilibria and arbitrary collisionality regime". *Physics of Plasmas*, 9(12):5140–5140, 2002.

[9] A. J. van der Schaft and B. M. Maschke. Hamiltonian formulation of distributed–parameter systems with boundary energy flow. *Journal of Geometry and Physics*, 42(1–2):166–194, 2002.

[10] B. Vincent, N. Hudon, L. Lefèvre, and D. Dochain. Port–Hamiltonian observer design for plasma profile estimation in tokamaks. *IFAC–PapersOnLine*, 49(24):93 – 98, 2016. 2th IFAC Workshop on Thermodynamic Foundations for a Mathematical Systems Theory TFMST.

[11] B. Vincent, N. Hudon, L. Lefèvre, and D. Dochain. Burning magneto–hydrodynamics plasmas model: A port–based modelling approach. *IFAC–PapersOnLine*, 50:13580 – 13585, 2017.

[12] B. Vincent, T. Vu, N. Hudon, L. Lefèvre, and D. Dochain. Port–Hamiltonian modeling and reduction of a burning plasma system. *IFAC–PapersOnLine*, 51(3):68 – 73, 2018. 6th IFAC Workshop on Lagrangian and Hamiltonian Methods for Nonlinear Control LHMNC 2018.

[13] N. M. Trang Vu, L. Lefèvre, and B. Maschke. A structured control model for the thermo–magneto–hydrodynamics of plasmas in tokamaks. *Mathematical and Computer Modelling of Dynamical Systems*, 22(3):181–206, 2016.

[14] N. M. Trang Vu, L. Lefèvre, R. Nouailletas, and S. Brémond. Symplectic spatial integration schemes for systems of balance equations. *Journal of Process Control*, 51:1 – 17, 2017.

[15] N. M. Trang Vu, R. Nouailletas, E. Maljaars, F. Felici, and O. Sauter. Plasma internal profile control using IDA–PBC: Application to TCV. *Fusion Engineering and Design*, 2017. In Press.

[16] J. Wesson and D. J. Campbell. *Tokamaks*. Clarendon Press, New York, 2004.

[17] E. Witrant, E. Joffrin, S. Brémond, G. Giruzzi, D. Mazon, O. Barana, and P. Moreau. A control–oriented model of the current profile in tokamak plasma. *Plasma Physics and Controlled Fusion*, 49(7):1075–1105, 2007.